Journal of Inflammation Research

Dovepress
open access to scientific and medical research

Open Access Full Text Article

ORIGINAL RESEARCH

Pretreated MSCs with IronQ Transplantation Attenuate Microglia Neuroinflammation via the cGAS-STING Signaling Pathway

Guoqiang Yang[1–3], Jiraporn Kantapan[3], Maryam Mazhar[4,5], Qiongdan Hu[1,5,6], Xue Bai[5,7], Yuanxia Zou[1,3], Honglian Wang[1], Sijin Yang[4,5], Li Wang[1,5], Nathupakorn Dechsupa[3]

[1]Research Center for Integrated Chinese and Western Medicine, the Affiliated Traditional Chinese Medicine Hospital of Southwest Medical University, Luzhou, People's Republic of China; [2]Acupuncture and Rehabilitation Department, the Affiliated Traditional Chinese Medicine Hospital of Southwest Medical University, Luzhou, People's Republic of China; [3]Molecular Imaging and Therapy Research Unit, Department of Radiologic Technology, Faculty of Associated Medical Sciences, Chiang Mai University, Chiang Mai, Thailand; [4]National Traditional Chinese Medicine Clinical Research Base and Drug Research Center of the Affiliated Traditional Chinese Medicine Hospital of Southwest Medical University, Luzhou, People's Republic of China; [5]Institute of Integrated Chinese and Western Medicine, Southwest Medical University, Luzhou, People's Republic of China; [6]Department of Medical Technology, Faculty of Associated Medical Sciences, Chiang Mai University, Chiang Mai, Thailand; [7]Department of Neurology and National Traditional Chinese Medicine Clinical Research Base, the Affiliated Traditional Chinese Medicine Hospital of Southwest Medical University, Luzhou, People's Republic of China

Correspondence: Li Wang; Nathupakorn Dechsupa, Email wangli120@swmu.edu.cn; nathupakorn.d@cmu.ac.th

Background: Intracerebral hemorrhage (ICH), a devastating form of stroke, is characterized by elevated morbidity and mortality rates. Neuroinflammation is a common occurrence following ICH. Mesenchymal stem cells (MSCs) have exhibited potential in treating brain diseases due to their anti-inflammatory properties. However, the therapeutic efficacy of MSCs is limited by the intense inflammatory response at the transplantation site in ICH. Hence, enhancing the function of transplanted MSCs holds considerable promise as a therapeutic strategy for ICH. Notably, the iron-quercetin complex (IronQ), a metal-quercetin complex synthesized through coordination chemistry, has garnered significant attention for its biomedical applications. In our previous studies, we have observed that IronQ exerts stimulatory effects on cell growth, notably enhancing the survival and viability of peripheral blood mononuclear cells (PBMCs) and MSCs. This study aimed to evaluate the effects of pretreated MSCs with IronQ on neuroinflammation and elucidate its underlying mechanisms.

Methods: The ICH mice were induced by injecting the collagenase I solution into the right brain caudate nucleus. After 24 hours, the ICH mice were randomly divided into four subgroups, the model group (Model), quercetin group (Quercetin), MSCs group (MSCs), and pretreated MSCs with IronQ group (MSCs+IronQ). Neurological deficits were re-evaluated on day 3, and brain samples were collected for further analysis. TUNEL staining was performed to assess cell DNA damage, and the protein expression levels of inflammatory factors and the cGAS-STING signaling pathway were investigated and analyzed.

Results: Pretreated MSCs with IronQ effectively mitigate neurological deficits and reduce neuronal inflammation by modulating the microglial polarization. Moreover, the pretreated MSCs with IronQ suppress the protein expression levels of the cGAS-STING signaling pathway.

Conclusion: These findings suggest that pretreated MSCs with IronQ demonstrate a synergistic effect in alleviating neuroinflammation, thereby improving neurological function, which is achieved through the inhibition of the cGAS-STING signaling pathway.

Keywords: mesenchymal stem cells, IronQ, intracerebral hemorrhage, cGAS/STING/NFκB, inflammatory response

Background

Intracerebral hemorrhage (ICH), a devastating subtype of stroke, is characterized by high morbidity and mortality rates, with nearly 5 million cases and over 2.8 million deaths worldwide.[1–5] Post-ICH, an extended hematoma results in primary brain injury (PBI), causing mass effects and the destruction of surrounding normal brain tissue.[6] Previous studies have demonstrated the feasibility of managing PBI through craniotomy and minimally invasive endoscopic approaches

Received: 14 December 2023
Accepted: 29 February 2024
Published: 13 March 2024

for hematoma evacuation in cases of ICH.[7] Subsequently, as ICH progresses, released debris, hemoglobin, iron, heme, and other blood components from the ruptured red blood cells within the hematoma trigger secondary brain injury (SBI). This initiates a cascade of pathological events, encompassing neuroinflammation, brain edema, demyelination, axonal damage, neuronal death, oxidative stress, and disruption of the blood-brain barrier (BBB).[3,8–12] In recent years, there has been an increasing focus on comprehending the mechanisms and therapeutic strategies targeting SBI-mediated neuroinflammation in the context of ICH.[13,14] Nevertheless, the underlying mechanisms of SBI-induced neuroinflammation following ICH remain not fully understood.

Mesenchymal stem cells (MSCs), known for their anti-inflammatory properties, have emerged as a promising therapeutic option for various brain diseases.[15–18] However, the therapeutic efficacy of MSCs is impeded by the activated microglia-induced neuroinflammation, resulting in a diminished survival rate of MSCs at the site of a brain hemorrhage.[19,20] Moreover, numerous reports have indicated that traditional Chinese medicine, particularly quercetin, can modulate the proliferation and differentiation of MSCs.[21,22] Quercetin, a flavonoid present in various herbs, fruits, and vegetables, has been demonstrated to diminish neuronal injury and facilitate brain damage recovery by attenuating neuroinflammation.[23] Several studies have reported that quercetin can modulate cellular functions, such as proliferation and migration.[19,23] However, quercetin's low water solubility, restricted bioavailability, and chemical instability have presented challenges to its efficacious utilization in biomedical applications.[24,25] To overcome these limitations, our research team has synthesized the iron-quercetin complex (IronQ), which demonstrates enhanced water solubility, improved bioactivity, and potential for tracking peripheral blood mononuclear cells (PBMCs) and MSCs.[26–28] Based on this premise, we hypothesized that the administration of MSCs with IronQ could improve outcomes in ICH mice and sought to investigate the underlying mechanisms involved.

Microglia, serving as the resident macrophages of the central nervous system (CNS), play a pivotal role in the innate immune response following ICH. The release of inflammatory factors by activated microglia contributes to the amplification of the inflammatory response in diverse brain diseases.[29] The production of interleukin-6 (IL-6) and tumor necrosis factor α (TNF-α) after ICH is primarily attributed to microglia activation.[20] Microglia/macrophages can assume distinct phenotypes, namely M1 and M2, based on their gene and protein expression profiles. The M1 phenotype exacerbates injury, whereas the M2 phenotype contributes to tissue repair.[30] After ICH, two distinct subtypes of cells exist in the brain tissue, manifesting dynamic changes in their functions, which can either contribute to tissue repair or exacerbate injury. The cyclic GMP-AMP (cGMP-AMP) synthase (cGAS) and its downstream cGMP-AMP receptor stimulator of interferon genes (STING) detect disease-producing DNA, initiating an inflammatory response. This suggests cGAS-STING axis as a pivotal signaling pathway in autoimmunity and inflammatory responses.[31] Several studies have presented compelling evidence indicating that prolonged activation of the cGAS-STING signaling pathway in the CNS can have detrimental effects on normal brain function.[32] In recent years, there has been extensive research devoted to exploring the neuroinflammatory response linked with the cGAS-STING signaling axis in neurodegenerative diseases, including Alzheimer's disease (AD), and ischemic stroke.[33–35] These studies have illuminated the role of the cGAS-STING pathway in the pathogenesis of these conditions and underscored its potential as a therapeutic target. However, the precise effect and underlying mechanism of the cGAS-STING signaling pathway in the context of hemorrhagic brain conditions remain inadequately understood. Further research is needed to elucidate the role of this signaling pathway in hemorrhagic brain injury and its potential implications for therapeutic interventions.

In this study, we evaluated the neurological deficits, DNA damage, and inflammatory response in neuronal cells following the transplantation of preconditioned MSCs with IronQ in ICH mice. Additionally, we investigated the protein expression levels of the cGAS-STING signaling axis to gain insights into its involvement in the observed effects.

Materials and Methods

The Synthesis of IronQ Complex

The IronQ complex was synthesized following the methodology described in our previous study.[26] Shortly, stirring quercetin hydrate (0.0050 moles) (Sigma, USA) in a round bottle with 500 mL HPLC-methanol (Sigma, USA) until complete dissolution, the solution's color shifted yellow. Then, the PH of mixed solution was gradually modified to 12

using a NaOH solution. Subsequently, Iron (III) chloride (Sigma, USA) solution was freshly prepared by dissolving 0.0025 moles of Iron (III) chloride in 500 mL of ultrapure water (up water) to integrate with the quercetin solution resulting in a dark yellow mixture, which was subsequently incubated for 2 hours at 60°C under a continued stirring. After that, the total solution was filtered and evaporated to dryness. The resulting dark powder was collected and reserved it at room temperature (RT) in a drying apparatus, protected from the light.

Animals

Sixty male wild-type mice (C57BL/6), aged 8–9 weeks and weighing between 22 and 25 g, were obtained from Tengxin Biotechnology Co., Ltd (Chongqing, China). The mice were housed in a temperature-controlled room (23 ± 2 °C) with consistent animal housing conditions, including relative humidity (65 ± 5%), a 12:12-hour light-dark cycle, and ad libitum access to water and food. The approach to utilizing the mice adhered to the Guidance Suggestions for the Care and Use of Laboratory Animals established by the Ministry of Science and Technology in China. The animal protocol was authorized by the Animal Ethical Committee of the Animal Center of Southwest Medical University (Luzhou, Sichuan), and the approval number is 20,220,526–002. The optimized experimental approaches were implemented to minimize the discomfort of the experimental animals. The experimental mice were randomly divided into six groups, comprising the sham group (Sham), the model group (Model), MSCs group (MSCs), quercetin group (Quercetin), IronQ-pretreated MSCs group (MSCs+IronQ), and control group with IronQ-pretreated MSCs (MSCs+IronQC). Each group was subjected to one of the following five different processing methods, as depicted in Figure 1A.

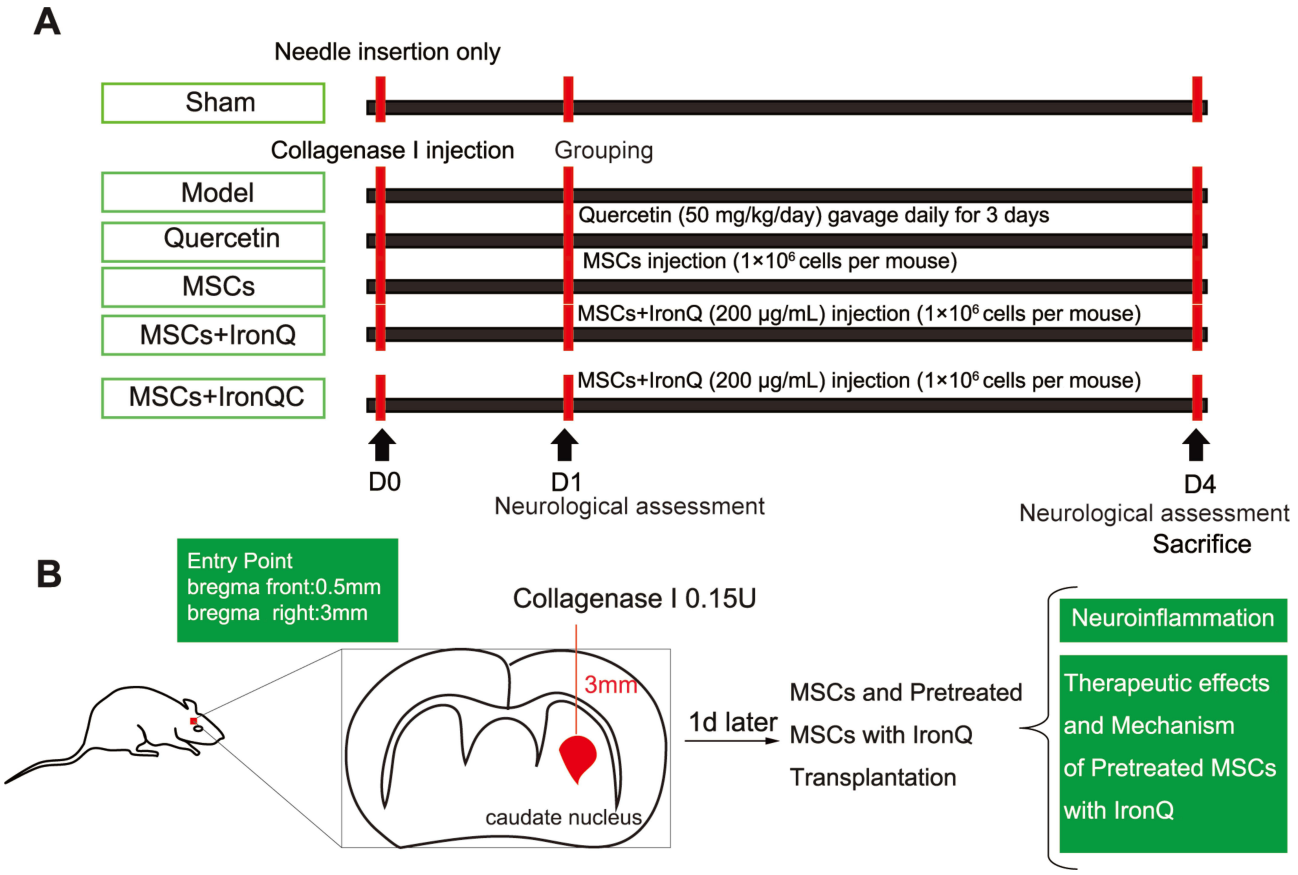

Figure 1 Abstract graphics of the experimental protocols. (**A**) Grouping, treatment procedures, and a concise timeline for experimental mice. (**B**) A schematic diagram of the ICH mice administered with MSCs and pretreated MSCs with IronQ.

Intracerebral Hemorrhage Mice Model

The ICH animal model was established following the methodology outlined in our previous study.[28,36] Shortly, anesthetized mice were secured by immobilizing the bilateral external ear hilum and incisor to a stereotaxic apparatus. The anterior and posterior fontanels were positioned at the horizontal plane to ensure stability. The scalp was dissected sagittally for approximately 1 cm to expose the anterior fontanelle by utilizing 30% H_2O_2. 1 μL solution (0.15 U/μL) of collagenase I (C8140, Solarbio, China) dissolved in 0.9% normal saline was taken by a microsyringe (1 μL, Shang Hai Gao Ge). A hole (1 mm in diameter) was drilled on the right calvaria bone at the lateral and anterior of the anterior fontanelle, with distances of 2.5 mm and 0.2 mm, respectively. The microsyringe, positioned on the stereotaxic apparatus, was carefully inserted into the brain tissue (caudate nucleus) to a depth of 3 mm from the drilled hole. Subsequently, the collagenase I solution was gradually infused using the microsyringe (Figure 1B). The skin was sutured after the drilled hole was closed using bone wax. The mice in the Sham underwent the same procedure, except that the collagenase I solution was not infused. The mice in the MSCs+IronQC were only injected with the pretreated MSCs with IronQ. In accordance with the previous study, mice in the Quercetin received quercetin administration at a dosage of 50 mg/kg/day via gastrointestinal drug delivery.[19,23] The abstract definitions of the experimental procedures are shown in Figure 1.

Neurological Score and Balance Beam Test

As cited above, neurobehavioral functions were blindly evaluated 1 day after ICH using the modified Garcia.[37,38] The modified Garcia test consists of 6 subtests with a total score of 18, including assessments of spontaneous movement, limb symmetry, forward extension, climbing ability, body proprioception, and tentacle feedback. For the beam balance test, mice were placed on a 2 cm wide beam and allowed to walk on it. This latency duration for the mice to reach the terminal home cage was documented. The maximum observation period allowed was 1 minute. Additionally, the number of paw slips was recorded, and the overall performance of the mice on the beam was assessed the according to the scoring criteria. All mice underwent conditioning and training on the balance beam two days before the initiation of the mice ICH induction experiment, as described in our previous study.[39]

Culture and Identification of MSCs

The procedures for obtaining MSCs were carried out as previously described.[28,40] In brief, the tibias and femurs were obtained from 10 healthy male mice under sterile conditions. Next, the muscle tissue surrounding the bone was meticulously removed using a scissor and tweezer, ensuring not to damage the bone structure. Subsequently, the bones were immersed in 75% alcohol for 30 seconds and then washed three times (1 minute each) with sterile 0.01 M phosphate-buffered saline (PBS, pH = 7.4). The bones were crushed, and the resulting fragments repeatedly were repeatedly washed with Dulbecco's modified eagle medium (DMEM, Gibco, USA) to obtain a cell suspension. The cell suspension was then centrifuged and the obtained cells were suspended. Subsequently, the cells were cultured in DMEM supplemented with 10% fetal bovine serum (FBS, Gibco, USA) and 1% penicillin/streptomycin (C0222, Beyotime Biotechnology, China), and incubated at 37°C in a humidified atmosphere containing 5% CO_2. The cultured cells from the third passage were used in the subsequent experiments. The cells were characterized using surface marker protein antibodies for MSCs, including CD90, CD105, CD 11b, and CD45 (Bioscience, USA), assessed via flow cytometry (BD FACSCanto II, BD Biosciences, USA).

Pretreated MSCs with IronQ

MSCs (1×10^6 cells) were seeded in a 10-cm culture plate with the previously mentioned culture medium. Once the MSCs adhered to the plate surface, dissolved IronQ in sterile ultrapure (up) water at a concentration of 1000 μg/mL was added to the 10-cm culture plate to achieve at a final concentration of 200 μg/mL. The MSCs with IronQ were then further incubated at 37°C for 24 hours in a humidified incubator with 5% CO_2.[28]

Measurement of Reactive Oxidative Stress (ROS) Level

Human neuroblastoma SH-SY5Y cell line was obtained from the Chinese Academy of Science (Shanghai, China), seeded into a 6-well plate with DME/F12 (1:1) (Invitrogen, USA) supplemented with 10% FBS (Gibco, USA), 1%NEAA (Invitrogen, USA), 1% sodium pyruvate (Invitrogen, USA), 1%Gluta-max (35,050,061, Invitrogen, USA), 1%NEAA (Invitrogen, USA), and 1%penicillin/streptomycin (Beyotime, China), and cultured at 37°C in a humid atmosphere of 5% CO_2-incubator. The SH-SY5Y cells were pretreated with or without IronQ for 24 hours. Subsequently, the media were removed, and the cells were further cultured in their original media supplemented with 100 μM H_2O_2 (except for control) for an additional 12 hours. Then, the cells were assessed using a ROS detection kit (Beyotime, China) following the manufacturer's instructions. Fluorescence intensity was quantified by flow cytometry (BD FACSCanto II, BD Biosciences, USA) at an excitation wavelength of 488 nm and an emission wavelength of 525 nm.

Transplantation of MSCs and Pretreated MSCs with IronQ

MSCs at passages 3–6, along with their pretreated form with IronQ, were utilized in the subsequent experiments. The cells were collected and the cell concentration was adjusted to 5×10^7 cells per mL in PBS. Then a 20 μL cells suspension containing 10^6 cells was drawn into the same volume microsyringe and infiltrated into the original site for ICH mice (location: bregma right: 3 mm; bregma front: 0.2 mm; depth: 3 mm) at an injection speed of 2 μL/min in the mice of MSCs, MSCs+IronQ, and MSCs+IronQC, respectively, after the ICH mice model was successfully established. The skin was sutured and disinfected.[28]

Terminal Deoxynucleotide Transferase dUTP Nick-End Labeling (Tunel) Staining

Tunel staining was described to assess neuronal apoptosis in the caudate nucleus (perihematoma) following ICH, as described in a previous report.[41] Briefly, after myocardial perfusion with 0.9% normal saline and 4% paraformaldehyde in PBS for deep anesthesia in mice, brain samples were removed and immersed in the same formaldehyde solution for further fixation. Subsequently, the samples were embedded in paraffin. Neuronal apoptosis was assessed using a One-step TUNEL In Situ Apoptosis Assay Kit (Green, AF488) (E-CK-A321, Elabscience, China), following the manufacturer's protocol. Images were captured using an orthotopic fluorescence microscope (DM4B, Leica, Germany).

Immunofluorescence

Immunofluorescence (IF) was conducted following the methodology described in previous literature.[28,42] Shortly, after transcardially using 0.9% normal saline and 4% paraformaldehyde in PBS for mice in-depth anesthesia, the brain samples were collected, and post-fixed. Subsequently, the samples were dehydrated and embedded in an optimal cutting temperature compound (OCT). Next, the brain tissue was sliced into 4-μm sections at the side of the caudate nucleus using a freezing microtome (CM1950, Leica, Germany). Frozen sections of brain tissue were treated with 0.3% Triton X-100, followed by blocking with 5% BSA at 37°C for 1 hour. Subsequently, the sections were incubated with primary antibodies, including rabbit anti-NeuN (CST, USA, diluted 1:100), Iba-1 (Abcam, USA, diluted 1:100), rabbit anti-CD80 (Proteintech, USA, diluted 1:100), rabbit anti-CD86 (Proteintech, USA, diluted 1:100), rabbit anti-CD206 (Proteintech, USA, diluted 1:100), rabbit anti-Arg-1 (Proteintech, USA, diluted 1:100), mouse anti-TNF-α (Santa Cruz, USA, diluted 1:100), mouse anti-IL-6 (Santa Cruz, USA, diluted 1:100), rabbit anti-cGAS (CST, USA, diluted 1:100), and rabbit anti-STING (Proteintech, USA, diluted 1:100) overnight under humidified conditions at 4°C and then incubated with Alexa Fluor™ 555 goat anti-rabbit IgG (Invitrogen, USA, diluted 1:1000), Alexa Fluor® 555 goat anti-mouse secondary IgG (Life Technologies, USA, diluted 1:1000), Alexa Fluor™ 488 conjugated anti-rabbit IgG (Invitrogen, USA, diluted 1:1000), and Alexa Fluor™ 488 conjugated anti-mouse IgG (Invitrogen, USA, diluted 1:1000) at RT for 1 hour. The images were captured using an orthotopic fluorescence microscope (DM4B, Leica, Germany).

Western Blot

Brain tissue was rapidly obtained and isolated into ipsilateral brain hemispheres after deep anesthesia of mice in different groups. The samples were homogenized, and the protein supernatants were harvested by centrifugation. Next, the total

protein concentration of brain samples in different groups was determined using the bicinchoninic acid (BCA) protein assay (Beyotime, China). Equal amounts of protein samples (50 μg) were loaded onto 10–12% sodium dodecyl sulfate-polyacrylamide gel (SDS-PAGE) for protein electrophoresis. Subsequently, the proteins were transferred to polyvinylidene fluoride (PVDF) membranes, which were then incubated with the first primary antibodies (CD80, CD86, CD206, Arg-1, IL-6, TNF-α, cGAS, STING, NFκB, p-NFκB-p65, and GAPDH, diluted 1:1000) at 4 °C overnight.[28] Following the primary antibody incubation, the membranes were further incubated with HRP-conjugated Donkey anti-rabbit/ mouse IgG (Thermo, USA, diluted 1: 1000) at RT for 1 hour. Then, the membranes were exposed to an Image-Quant ECL Imager using the enhanced chemiluminescence (ECL) solution (Vazyme, China). The relative protein levels were calculated by referencing the corresponding amount of GAPDH using Image J software.

Statistical Analysis

Parametric data were analyzed and presented as the mean ± standard error of the mean (SEM) using GraphPad Prism 8 software. The significant difference between multiple means was assessed using one-way Analysis of Variance (ANOVA) followed by a post hoc test.

Results

Pretreated MSCs with IronQ Attenuated the Neurological Deficits and DNA Damage

One day after inducing the ICH model, the balance beam and modified Garcia tests were employed to assess the neurological deficits in the experimental subjects. Figure 2A showed that on day 1 (1d), the ICH mice exhibited similar neurological scores, indicating that their baseline neurological condition was comparable at the beginning of the study ($P > 0.05$). When administering three different therapies, namely MSCs+IronQ, MSCs, and Quercetin, to the ICH mice, significant improvements in the scores of neurological deficits were observed compared to the Model at day 3 (3d). In Figure 2B, the results of TUNEL staining in different groups are presented, with the green color indicating DNA damage. The TUNEL staining performed at 3d after ICH showed a higher presence of DNA damage in the perihematoma in the mice from the Model compared to the mice in MSCs+IronQC and Sham. However, all three therapies demonstrated the ability to reduce the degree of DNA damage. Furthermore, it was observed that the pretreated MSCs with IronQ exhibited a greater anti-DNA damage effect when compared to the administration of quercetin via gavage and MSCs transplantation alone.

Identification of Pretreated MSCs with IronQ at Different Time Points

The original MSCs extracted from the tibias and femurs of mice were cultured and subsequently passed to the third passage (Figure 3A). The expression profiles of surface antigens were analyzed, revealing the presence of positive markers CD29 (99.5%) and CD105 (89.3%) and the absence of negative markers CD11b (13.8%) and CD45 (0.9%) (Figure 2C). The cluster growth of MSCs at passages 3–6 can be observed under an inverted phase contrast microscope (Figure 2A). When incubated MSCs with IronQ (Figure 3B) (200 μg/mL) for 1 day and 3 days in a humidified atmosphere incubator with 5% CO_2 at 37 °C, the surface antigens on IronQ-preconditioned MSCs exhibited slight difference compared to non-IronQ-preconditioned MSCs (Figure 3D–E). The results showed that CD11b exhibited an increasing trend with the extension of IronQ preconditioning time on MSCs.

Pretreated MSCs with IronQ Attenuated the H_2O_2-Induced ROS of SH-SY5Y Cells

H_2O_2 is known to induce the generation of ROS and can be toxic to cells. In order to investigate whether pretreated MSCs with IronQ can protect SH-SY5Y cells by reducing ROS accumulation, the intracellular ROS levels were measured using DCFH-DA probes. This was accomplished by exposing the SH-SY5Y cells to conditioned medium (CM) obtained from pretreated MSCs with IronQ for 24 hours. The fluorescence intensity of intracellular ROS was measured using flow cytometry (Figure 4). The results revealed a significant increase in intracellular ROS levels following H_2O_2 stimulation. However, when the CM of pretreated MSCs with IronQ (200 μg/mL) was utilized to treat H_2O_2-activated SH-SY5Y cells, a noticeable reduction in intracellular ROS levels was observed.

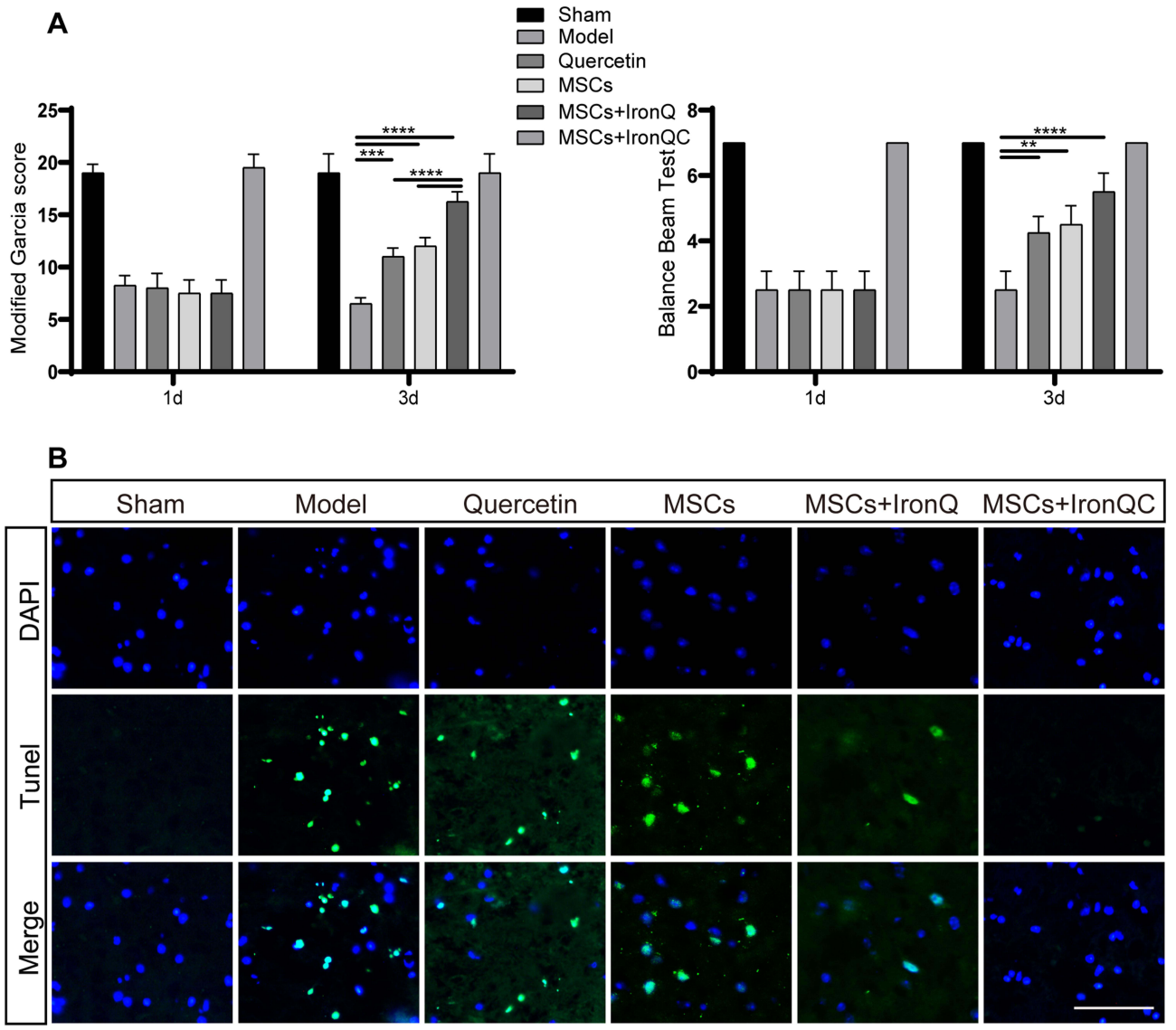

Figure 2 The administration of pretreated MSCs with IronQ attenuated neurological deficits and DNA damage. (**A**) The results from the Modified Garcia and beam balance tests indicated that the administration of pretreated MSCs with IronQ significantly reduced neurological deficits in ICH mice at 3 days post-treatment. (**B**) The results of Tunel staining demonstrated that there were minimal DNA damage cells observed in the mice treated with MSCs+IronQ compared to the mice in the Model and the other two therapy groups at 3 days post-treatment. Scale bar = 100 μm. (n = 5 per group; ** $p< 0.01$, ***$p< 0.001$, and ****$P < 0.0001$).

Pretreated MSCs with IronQ Decreased Neuroinflammation in Mice Following ICH

Figure 5 presents the results of double immunofluorescent staining, specifically between NeuN (a neuronal marker) and inflammatory factors, in various groups. Particularly, in Figure 5A and B, a higher protein expression of inflammatory factors, such as IL-6 and TNF-α, is observed on neuronal cells in the ICH mice of the Model compared to the mice in the MSCs+IronQC and Sham. The therapies involving quercetin gavage and MSCs injection in situ were found to decrease the protein expression levels of inflammatory factors on neuronal cells. However, the transplantation of pretreated MSCs with IronQ downregulated the inflammatory factors more significantly than the other two therapies.

Pretreated MSCs with IronQ Enhanced the Transition to the Neuroprotective M2 Microglial Phenotype

Figure 6 shows double immunofluorescent staining results between microglia (Iba-1) and its polarization markers (M1: CD80, CD86; M2: CD206, Arg-1), along with the Western blot results of microglial polarization markers in different

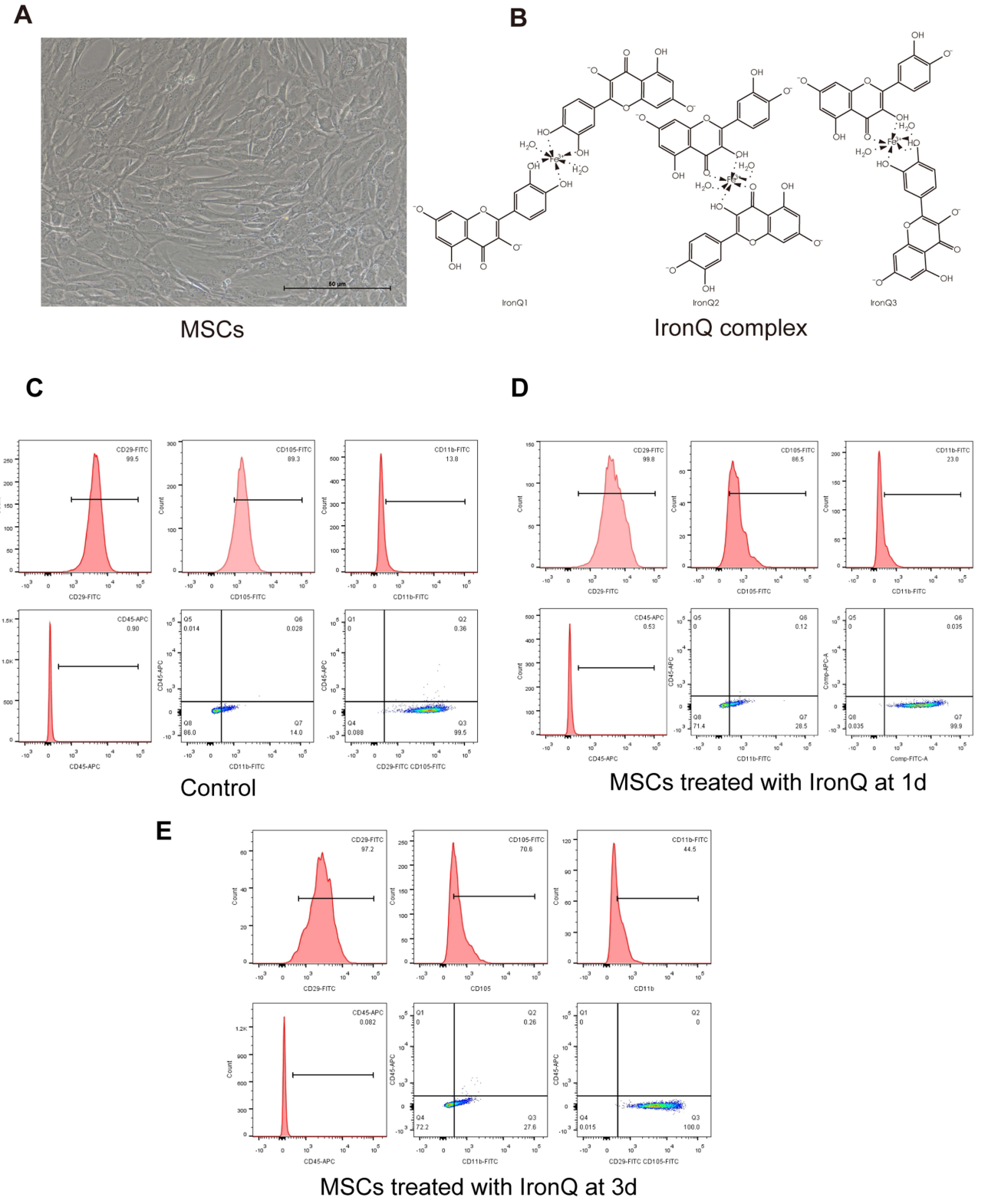

Figure 3 IronQ-preconditioned MSCs sustain the stem cell properties. (**A**) Vortex-like growth of MSCs at passages 3–6. Scale bar = 50μm. (**B**) Three possible structures of IronQ complex. (**C**–**E**) The expression profiles of surface antigens on IronQ-preconditioned MSCs were analyzed at different time points to evaluate any changes in their surface antigen expression.

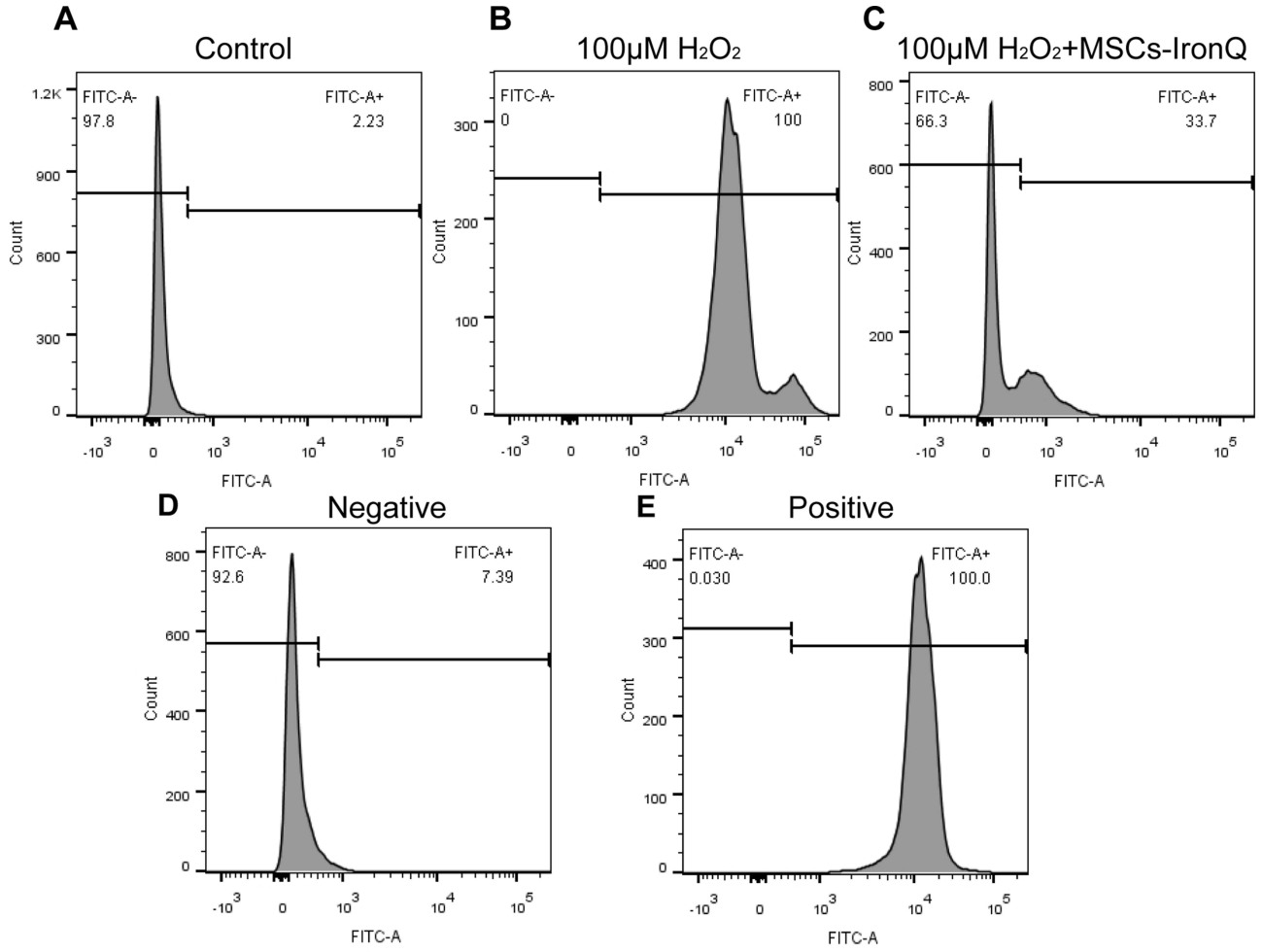

Figure 4 Pretreated MSCs with IronQ hindered H_2O_2-mediated intracellular ROS accumulation in SH-SY5Y cells. (**A**–**E**) The fluorescence intensity of intracellular ROS was quantified using flow cytometry.

groups. Specifically, Figure 6A depicts the double staining showcasing microglial phenotype M1 and M2 with Iba-1. The Western blot results reveal that the quercetin gavage therapy augmented the protein expression levels of CD206 and Arg-1, while no discernible impact was observed on CD80 and CD86. The injection of MSCs led to enhanced protein expression levels of CD206 and Arg-1 and decreased CD80 and CD86 protein expression levels compared with quercetin gavage therapy. Moreover, the combined treatment resulted in significant downregulation of M1 markers and upregulation of M2 markers compared to quercetin gavage therapy alone. Additionally, the combined therapy significantly boosted CD206 protein expression level compared to MSCs transplantation alone. Therefore, the transplantation of pretreated MSCs with IronQ demonstrated a synergistic effect in enhancing the microglial transformation into the M2 phenotype.

Pretreated MSCs with IronQ Downregulated Neuroinflammation by Regulating the cGAS-STING-NFκB Signal Axis

In Figure 7A and B, the co-expression of Iba-1 (a microglial marker) with cGAS and STING was assessed through immunofluorescence. In the Sham and MSCs+IronQC, no detectable co-expression of Iba-1 with cGAS and STING was observed based on immunofluorescent staining. However, following ICH induction, a uniform distribution of Iba-1 co-expression with cGAS and STING staining was observed in brain tissue. Interestingly, weak immunofluorescent staining of microglial cGAS and STING was also observed in all three treatment groups. Furthermore, the IronQ-pretreated

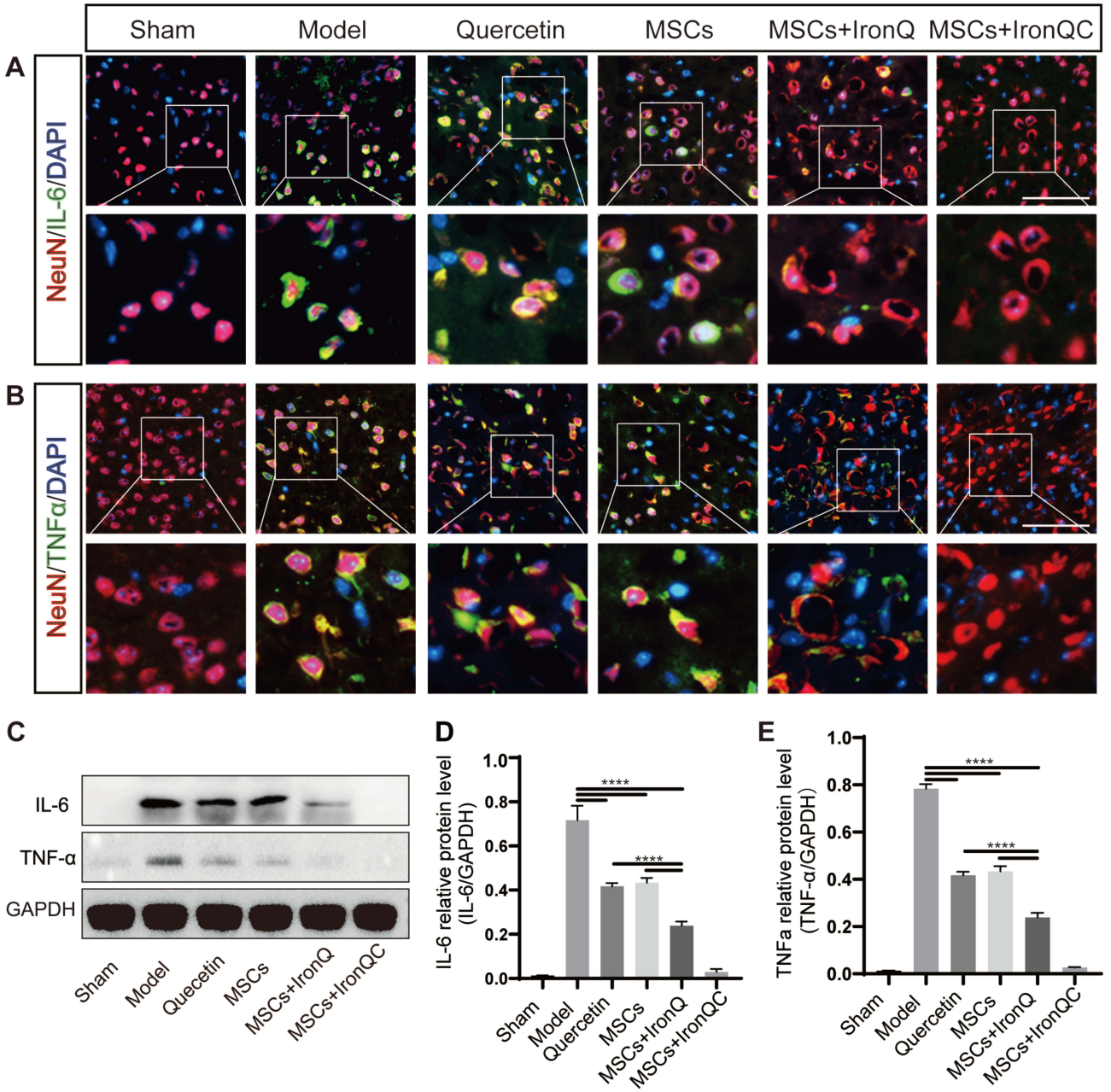

Figure 5 Pretreated MSCs with IronQ decreased neuroinflammation in mice with ICH. (**A** and **B**) Representative double immunofluorescent staining of inflammatory factors/NeuN in ipsilateral basal ganglia of mice after ICH (n = 5 per group). Scale bar = 100 μm. (**C**–**E**) The results and analysis of Western blotting in different groups revealed the protein expression levels of IL-6 and TNF-α in mouse brain tissue (n = 5 per group; ****$P < 0.0001$).

MSCs group exhibited fewer cells with positive staining for the co-expression of Iba-1 with cGAS and STING compared to the other two treatment groups. Figure 7C–F depict the protein expression levels and analysis of the cGAS-STING signal axis using Western blotting. The immunoblotting results demonstrate a significant increase in protein expression levels of cGAS, STING, and p-NFκB-p65 in brain tissue following ICH. However, therapies involving MSC transplantation, IronQ-pretreated MSCs, and quercetin gavage effectively inhibited their upregulation ($P < 0.0001$). The transplantation of MSCs resulted in a significant downregulation of protein expression levels of cGAS ($P < 0.05$) and STING ($P < 0.0001$) compared to quercetin gavage therapy. However, there was no significant difference in the protein expression levels of p-NFκB-p65 between the Quercetin and MSCs in mice. Furthermore, the transplantation of IronQ-pretreated

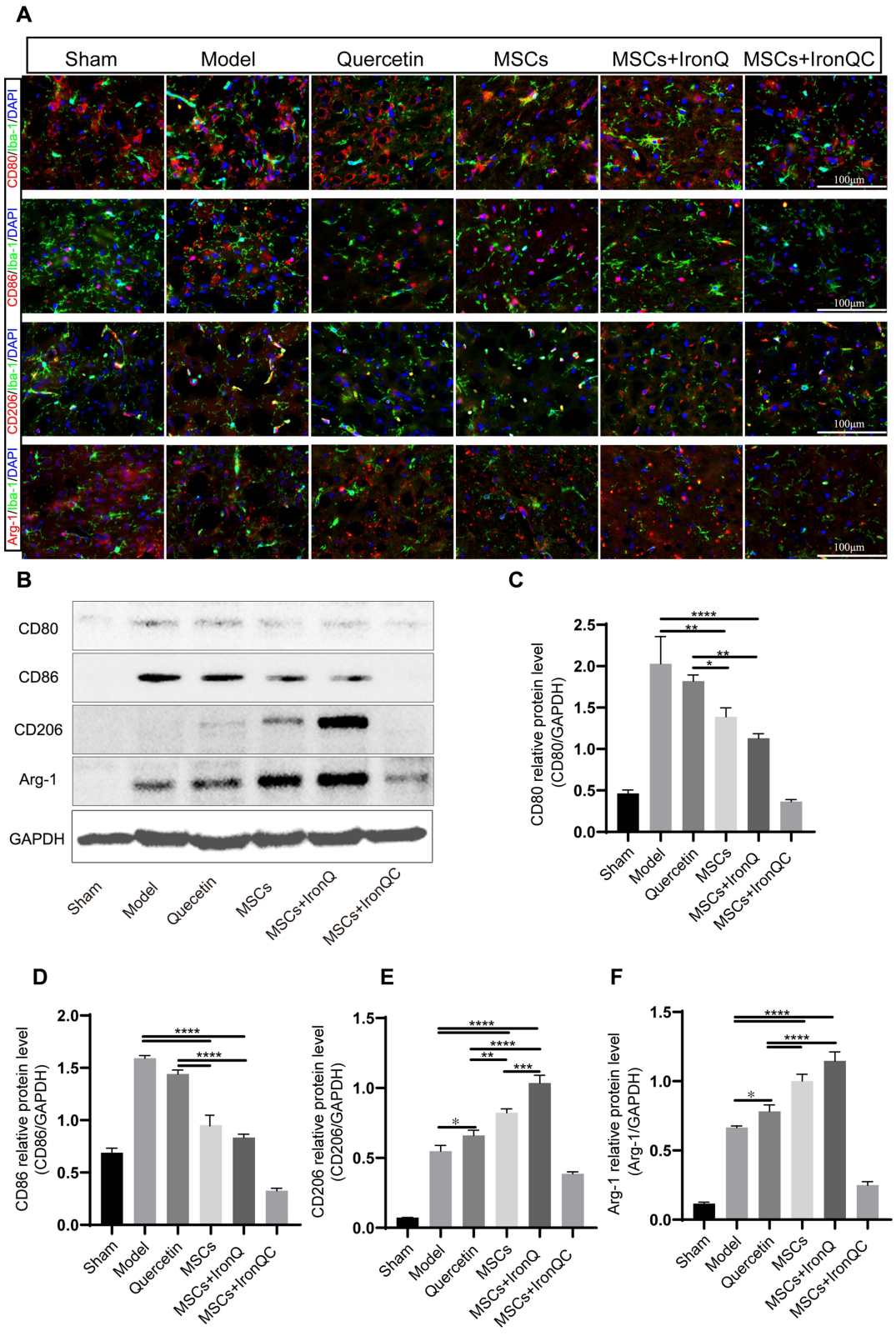

Figure 6 Pretreated MSCs with IronQ enhanced the transformation of the M2 microglial neuroprotective phenotype. (**A**) Representative double immunofluorescent staining of polarization marker/Iba-1 in ipsilateral basal ganglia of mice after ICH (n = 5 per group). Scale bar = 100 μm. (**B**–**F**) The results of Western blot in different groups revealed the protein expression levels of microglial polarization markers in mice brain tissue (n = 5 per group; **P* < 0.05, ** *p*< 0.01, ****p*< 0.001, and *****P* < 0.0001).

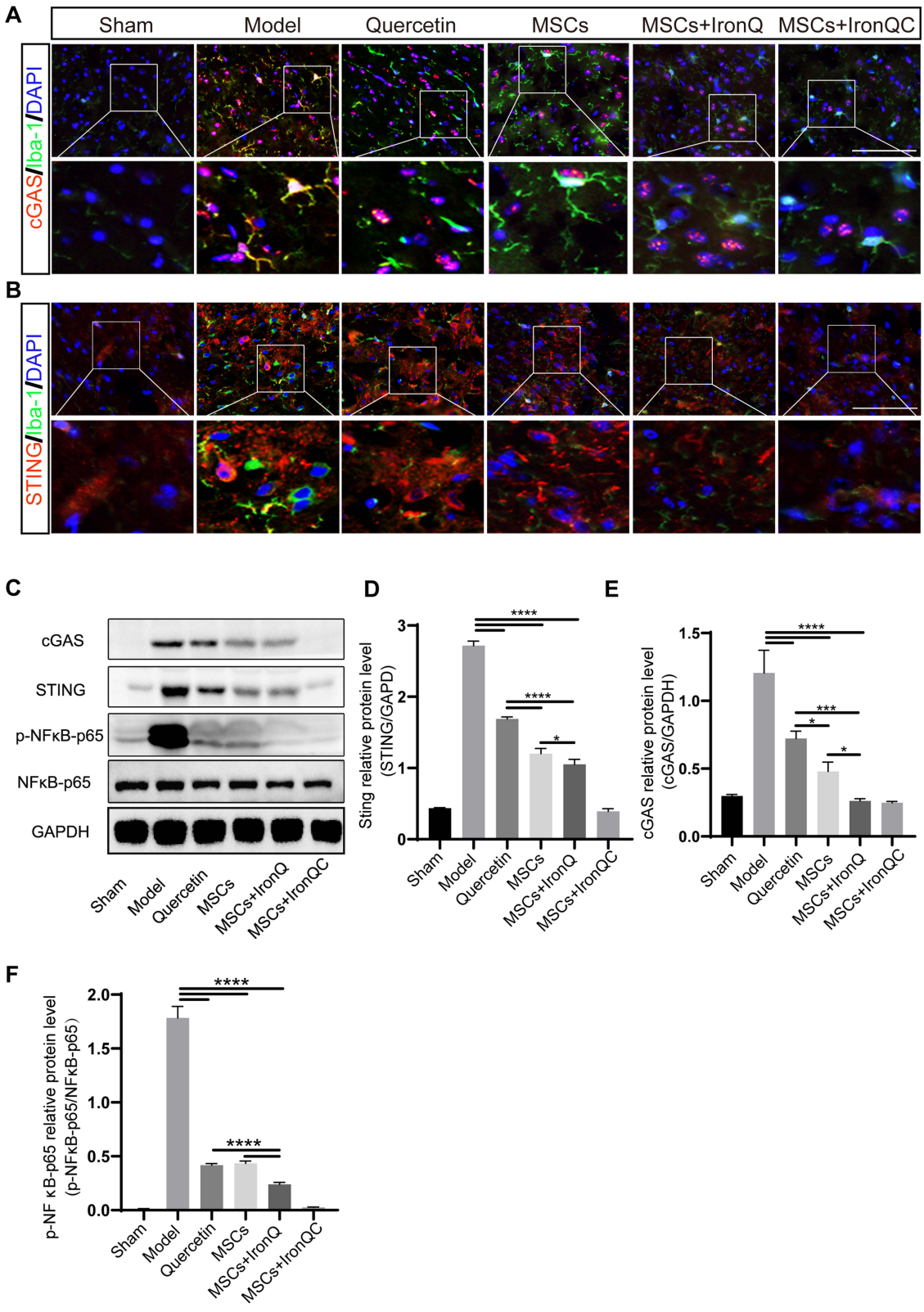

Figure 7 Pretreated MSCs with IronQ attenuated neuroinflammation by modulating the cGAS-STING-NFκB signal axis. (**A** and **B**) Immunofluorescence staining showed colocalization of Iba-1-positive microglia with cGAS and STING in mice after ICH (n = 5 per group). Scale bar = 100 μm. (**C**–**F**) The results and analysis of Western blot in different groups revealed the protein expression levels of cGAS, STING, and p-NFκB-p65 in mice brain tissue (n = 5 per group; **P* < 0.05, ****p*< 0.001, and *****P* < 0.0001).

MSCs exhibited a significant downregulation of cGAS, STING, and p-NFκB-p65 protein expression levels compared to MSC transplantation and quercetin gavage therapies ($P < 0.05$).

Discussion

Previous studies have provided substantial evidence supporting the beneficial effects of MSC transplantation on improving outcomes in ICH.[28] This study investigated the potential protective effects and underlying mechanisms of using IronQ complex to precondition MSCs as an innovative therapy for ICH in mice. Our findings revealed that IronQ-pretreated MSCs enhanced the transformation of microglia into an M2 phenotype, mitigating neurological impairment in the perihematomal tissue of ICH mice. These effects were achieved via the modulation of the cGAS-STING-NFκB signaling axis.

Neuroinflammation is pivotal in inducing cellular swelling and damage, as highlighted in a previous study.[43] Following hematoma formation, the components of blood cells within and surrounding the hematoma are released into the adjacent normal brain parenchyma, triggering an instantaneous inflammatory reaction by activated inflammatory cells within the brain tissue.[44] Microglia, as a key component in the innate immune system of brain tissue, can swiftly mobilize and activate in response to ICH-induced brain damage.[45,46] The abundance of M1 microglia cells can lead to neuronal damage via the secretion of pro-inflammatory cytokines and neurotoxic chemokines. Studies have demonstrated that MSCs possess the capability to induce the polarization of macrophages/microglia towards an M2 phenotype in CNS diseases by suppressing the secretion of inflammatory factors from microglia cells.[20,47] In our study, we observed that the combined treatment effectively downregulated the protein expression levels of microglial M1-phenotype markers while concomitantly increasing the expression levels of M2-phenotype markers. These findings indicate that the combined treatment modulates microglial polarization towards a neuroprotective phenotype, suggesting its potential neuroprotective function. Furthermore, we observed that the combined treatment reduced inflammation within the brain tissue following ICH, which aligned with the observed changes in microglial polarization.

Neuroinflammation in the brain is often accompanied by and contributes to neurodegeneration. The cGAS-STING signaling axis is a cytoplasmic pathway responsible for sensing double-stranded DNA (dsDNA) and plays a crucial role in detecting endogenous pathogenic DNA. It serves as a key mediator of neuroinflammation in various inflammatory brain disorders.[31,48,49] The role of cGAS in regulating DNA repair through its downstream effectors, including STING and NFκB signals, is associated with the pathogenesis of neuroinflammation in neurodegenerative diseases.[31,50,51] In this study, we observed that both MSCs and quercetin therapies effectively inhibited the inflammatory response following ICH, suppressing the cGAS-STING-NFκB signaling pathway. However, when pretreated MSCs with IronQ were transplanted into the hemorrhage site of ICH mice, the protein expression levels of inflammatory factors were markedly downregulated compared to the other two therapies. Moreover, the combined treatment involving pretreated MSCs with IronQ transplantation demonstrated a more significant inhibitory effect on the cGAS-STING-NFκB signaling pathway in mice with ICH compared to individual therapies using MSCs or quercetin. Therefore, these findings suggest that the transplantation of pretreated MSCs with IronQ may have a synergistic effect in modulating the cGAS-STING-NFκB signaling axis. This synergistic modulation has the potential to alleviate neuroinflammation-induced brain damage in mice following ICH.

The present study provides preliminary evidence supporting the involvement of the cGAS-STING-NFκB signaling axis in the inflammatory response observed in mice following ICH. Nevertheless, it is crucial to acknowledge the limitations of our study. Firstly, our study did not employ an ICH mice model with specific knockout of cGAS or STING in microglia. Secondly, we did not extensively investigate the precise effects of the classical cGAS-STING-NFκB signaling axis in ICH using the BV2 microglia cell line. Furthermore, our study did not include additional validation through the construction of cGAS and STING viruses. Therefore, further research is necessary to fully comprehend and explore the potential of the cGAS-STING-NFκB signaling axis as a promising target in ICH.

The findings of our study suggest that the cGAS-STING-NFκB signaling pathway becomes activated in mice following ICH, contributing to the exacerbation of neuroinflammation. However, treatment with IronQ-preconditioned MSCs effectively alleviates ICH-induced neuroinflammation by inhibiting the cGAS-STING-NFκB signaling axis. Based on the results of our study, the damaged DNA-sensing cGAS-STING-NFκB signaling pathway holds promise as a target

for the treating ICH-induced neuroinflammation. Additionally, our findings underscore the protective effect of IronQ-preconditioned MSCs, shedding light on the underlying molecular mechanisms and indicating potential for developing more targeted therapeutic interventions.

Conclusions

This study presents a promising therapeutic approach to enhance neurological recovery in mice with ICH. Our findings indicate that the transplanting IronQ-preconditioned MSCs may synergistically reduce the inflammatory response in brain tissue following ICH by modulating the cGAS-STING-NFκB signaling pathway. Overall, these findings suggest that this strategy holds potential as a valuable therapeutic intervention to ameliorate the neurological deficits associated with ICH.

Data Sharing Statement

The data that support the findings of this study are available from the corresponding author upon reasonable request.

Acknowledgment

A preprint has previously been published, entitled, "Yang G, Kantapan J, Mazhar M, Bai X, Zou Y, Wang H, et al. Mesenchymal stem cells transplantation combined with IronQ attenuates ICH-induced inflammation response via Mincle/Syk signaling pathway. Stem cell research and therapy. 2022. [Preprint]"

Author Contributions

All authors made a significant contribution to the work reported, whether that is in the conception, study design, execution, acquisition of data, analysis, and interpretation, or in all these areas; have drafted or written, or substantially revised or critically reviewed the article; have agreed on the journal to which the article will be submitted; reviewed and agreed on all versions of the article before submission, during revision, the final version accepted for publication, and any significant changes introduced at the proofing stage; and agree to take responsibility and be accountable for the contents of the article.

Funding

This work was supported by Chiang Mai University, Grant holder: Nathupakorn Dechsupa. This funding body took part in the design of the study and collection, analysis, and interpretation of data and in writing the manuscript. Other funding bodies, such as National Traditional Chinese Medicine Inheritance and Innovation Team (No: ZYYCXTD-C-202207), Sichuan Science and Technology Program (2022YFS0613), the Luzhou-Southwest Medical University Science and Technology Strategic Cooperation Project (2021LZXNYD-P04), Brain Disease Innovation Team of the Affiliated Traditional Chinese Medicine Hospital of Southwest Medical University (2022-CXTD-05), Sichuan Science and Technology Program (2022YFS0613), Luzhou City science and technology plan project (2022-JYJ-149), the Project of Southwest Medical University (2021ZKQN125), and the Project of Sichuan Provincial Administration of Traditional Chinese Medicine (2021MS499), have provided additional financial support for purchasing pieces of equipment and research materials for experiments. These fundings played no role in the design of the study and collection, analysis, and interpretation of data and in writing the manuscript.

Disclosure

The authors declare that they have no competing interests in this work.

References

1. Schrag M, Kirshner H. Management of intracerebral hemorrhage: JACC focus seminar. *J Am Coll Cardiol*. 2020;75(15):1819–1831. doi:10.1016/j.jacc.2019.10.066
2. Kirshner H, Schrag M. Management of intracerebral hemorrhage: update and future therapies. *Curr Neurol Neurosci Rep*. 2021;21(10):57. doi:10.1007/s11910-021-01144-9
3. Gross BA, Jankowitz BT, Friedlander RM. Cerebral intraparenchymal hemorrhage: a review. *JAMA*. 2019;321(13):1295–1303. doi:10.1001/jama.2019.2413

4. Hanley DF, Thompson RE, Rosenblum M, et al. Efficacy and safety of minimally invasive surgery with thrombolysis in intracerebral haemorrhage evacuation (MISTIE III): a randomised, controlled, open-label, blinded endpoint Phase 3 trial. *Lancet*. 2019;393(10175):1021–1032. doi:10.1016/S0140-6736(19)30195-3
5. Feigin VL, Lawes CM, Bennett DA, Barker-Collo SL, Parag V. Worldwide stroke incidence and early case fatality reported in 56 population-based studies: a systematic review. *Lancet Neurol*. 2009;8(4):355–369. doi:10.1016/S1474-4422(09)70025-0
6. Wu X, Luo J, Liu H, et al. Recombinant adiponectin peptide ameliorates brain injury following intracerebral hemorrhage by suppressing astrocyte-derived inflammation via the inhibition of drp1-mediated mitochondrial fission. *Transl Stroke Res*. 2020;11(5):924–939. doi:10.1007/s12975-019-00768-x
7. Adeoye O, Broderick JP. Advances in the management of intracerebral hemorrhage. *Nat Rev Neurol*. 2010;6(11):593–601. doi:10.1038/nrneurol.2010.146
8. Zhou Y, Wang Y, Wang J, Anne Stetler R, Yang Q-W. Inflammation in intracerebral hemorrhage: from mechanisms to clinical translation. *Prog Neurobiol*. 2014;115:25–44. doi:10.1016/j.pneurobio.2013.11.003
9. Xue M, Yong VW. Neuroinflammation in intracerebral haemorrhage: immunotherapies with potential for translation. *Lancet Neurol*. 2020;19(12):1023–1032. doi:10.1016/S1474-4422(20)30364-1
10. Bao WD, Zhou XT, Zhou LT, et al. Targeting miR-124/Ferroportin signaling ameliorated neuronal cell death through inhibiting apoptosis and ferroptosis in aged intracerebral hemorrhage murine model. *Aging Cell*. 2020;19(11):e13235. doi:10.1111/acel.13235
11. Gautam J, Xu L, Nirwane A, Nguyen B, Yao Y. Loss of mural cell-derived laminin aggravates hemorrhagic brain injury. *J Neuroinflammation*. 2020;17(1):103. doi:10.1186/s12974-020-01788-3
12. Tao C, Hu X, Li H, You C. White matter injury after intracerebral hemorrhage: pathophysiology and therapeutic strategies. *Front Hum Neurosci*. 2017;11:422. doi:10.3389/fnhum.2017.00422
13. Chen S, Peng J, Sherchan P, et al. TREM2 activation attenuates neuroinflammation and neuronal apoptosis via PI3K/Akt pathway after intracerebral hemorrhage in mice. *J Neuroinflammation*. 2020;17(1):168. doi:10.1186/s12974-020-01853-x
14. Wang Y, Tian M, Tan J, et al. Irisin ameliorates neuroinflammation and neuronal apoptosis through integrin alphaVbeta5/AMPK signaling pathway after intracerebral hemorrhage in mice. *J Neuroinflammation*. 2022;19(1):82. doi:10.1186/s12974-022-02438-6
15. Li G, Yu F, Lei T, et al. Bone marrow mesenchymal stem cell therapy in ischemic stroke: mechanisms of action and treatment optimization strategies. *Neural Regen Res*. 2016;11(6):1015–1024. doi:10.4103/1673-5374.184506
16. Lo Furno D, Mannino G, Giuffrida R. Functional role of mesenchymal stem cells in the treatment of chronic neurodegenerative diseases. *J Cell Physiol*. 2018;233(5):3982–3999. doi:10.1002/jcp.26192
17. Yang Y, Ye Y, Su X, He J, Bai W, He X. MSCs-derived exosomes and neuroinflammation, neurogenesis and therapy of traumatic brain injury. *Front Cell Neurosci*. 2017;11:55. doi:10.3389/fncel.2017.00055
18. Li Z, Li M, Shi SX, et al. Brain transforms natural killer cells that exacerbate brain edema after intracerebral hemorrhage. *J Exp Med*. 2020;217(12). doi:10.1084/jem.20200213
19. Tan RZ, Wang C, Deng C, et al. Quercetin protects against cisplatin-induced acute kidney injury by inhibiting Mincle/Syk/NF-kappaB signaling maintained macrophage inflammation. *Phytother Res*. 2020;34(1):139–152. doi:10.1002/ptr.6507
20. Yang G, Fan X, Mazhar M, et al. Mesenchymal stem cell application and its therapeutic mechanisms in intracerebral hemorrhage. *Front Cell Neurosci*. 2022;16:898497. doi:10.3389/fncel.2022.898497
21. Oh JH, Karadeniz F, Seo Y, Kong CS. Effect of quercetin 3-O-beta-D-galactopyranoside on the adipogenic and osteoblastogenic differentiation of human bone marrow-derived mesenchymal stromal cells. *Int J Mol Sci*. 2020;21(21):8044. doi:10.3390/ijms21218044
22. Chu J, Shi P, Yan W, et al. PEGylated graphene oxide-mediated quercetin-modified collagen hybrid scaffold for enhancement of MSCs differentiation potential and diabetic wound healing. *Nanoscale*. 2018;10(20):9547–9560. doi:10.1039/C8NR02538J
23. Zhang Y, Yi B, Ma J, et al. Quercetin promotes neuronal and behavioral recovery by suppressing inflammatory response and apoptosis in a rat model of intracerebral hemorrhage. *Neurochem Res*. 2015;40(1):195–203. doi:10.1007/s11064-014-1457-1
24. Wang Z, Ma Y, Jiang Y, et al. Encapsulating quercetin in cyclodextrin metal-organic frameworks improved its solubility and bioavailability. *J Sci Food Agric*. 2022;102(9):3887–3896. doi:10.1002/jsfa.11738
25. Chen H, Yao Y. Phytoglycogen improves the water solubility and Caco-2 monolayer permeation of quercetin. *Food Chem*. 2017;221:248–257. doi:10.1016/j.foodchem.2016.10.064
26. Papan P, Kantapan J, Sangthong P, Meepowpan P, Dechsupa N. Iron (III)-quercetin complex: synthesis, physicochemical characterization, and MRI cell tracking toward potential applications in regenerative medicine. *Contrast Media Mol*. 2020;2020:8877862. doi:10.1155/2020/8877862
27. Jiraporn Kantapan SD, Daowtak K, Roytrakul S, Sangthong P, Dechsupa N. Ex vivo expansion of EPCs derived from human peripheral blood mononuclear cells by iron-quercetin complex. *Biomed Res*. 2017;28(6):2730–2737.
28. Yang G, Kantapan J, Mazhar M, et al. Mesenchymal stem cells transplantation combined with IronQ attenuates ICH-induced inflammation response via Mincle/syk signaling pathway. *Stem Cell Res Ther*. 2023;14:1
29. Keep RF, Hua Y, Xi G. Intracerebral haemorrhage: mechanisms of injury and therapeutic targets. *Lancet Neurol*. 2012;11(8):720–731. doi:10.1016/S1474-4422(12)70104-7
30. Wang J, Xing H, Wan L, Jiang X, Wang C, Wu Y. Treatment targets for M2 microglia polarization in ischemic stroke. *Biomed Pharmacother*. 2018;105:518–525. doi:10.1016/j.biopha.2018.05.143
31. Hopfner KP, Hornung V. Molecular mechanisms and cellular functions of cGAS-STING signalling. *Nat Rev Mol Cell Biol*. 2020;21(9):1–22. doi:10.1038/s41580-020-0244-x
32. Paul BD, Snyder SH, Bohr VA. Signaling by cGAS-STING in neurodegeneration, neuroinflammation, and aging. *Trends Neurosci*. 2021;44(2):83–96. doi:10.1016/j.tins.2020.10.008
33. Jiang GL, Yang XL, Zhou HJ, et al. cGAS knockdown promotes microglial M2 polarization to alleviate neuroinflammation by inhibiting cGAS-STING signaling pathway in cerebral ischemic stroke. *Brain Res Bull*. 2021;171:183–195. doi:10.1016/j.brainresbull.2021.03.010
34. Hou Y, Wei Y, Lautrup S, et al. NAD(+) supplementation reduces neuroinflammation and cell senescence in a transgenic mouse model of Alzheimer's disease via cGAS-STING. *Proc Natl Acad Sci U S A*. 2021;118(37). doi:10.1073/pnas.2011226118
35. Jauhari A, Baranov SV, Suofu Y, et al. Melatonin inhibits cytosolic mitochondrial DNA-induced neuroinflammatory signaling in accelerated aging and neurodegeneration. *J Clin Invest*. 2020;130(6):3124–3136. doi:10.1172/JCI135026

36. Yang G, Zhu J, Zhan G, et al. Mesenchymal stem cell-derived neuron-like cell transplantation combined with electroacupuncture improves synaptic plasticity in rats with intracerebral hemorrhage via mTOR/p70S6K signaling. *Stem Cells Int*. 2022;2022:6450527. doi:10.1155/2022/6450527
37. Krafft PR, McBride DW, Lekic T, et al. Correlation between subacute sensorimotor deficits and brain edema in two mouse models of intracerebral hemorrhage. *Behav Brain Res*. 2014;264:151–160. doi:10.1016/j.bbr.2014.01.052
38. Fu S, Luo X, Wu X, et al. Activation of the Melanocortin-1 Receptor by NDP-MSH attenuates oxidative stress and neuronal apoptosis through PI3K/Akt/Nrf2 pathway after intracerebral hemorrhage in mice. *Oxid Med Cell Longev*. 2020;2020:8864100. doi:10.1155/2020/8864100
39. Mazhar M, Yang G, Mao L, et al. Zhilong huoxue tongyu capsules ameliorate early brain inflammatory injury induced by intracerebral hemorrhage via inhibition of canonical nfsmall ka, cyrillicbeta signalling pathway. *Front Pharmacol*. 2022;13:850060. doi:10.3389/fphar.2022.850060
40. Huang S, Xu L, Sun Y, Wu T, Wang K, Li G. An improved protocol for isolation and culture of mesenchymal stem cells from mouse bone marrow. *J Orthop Translat*. 2015;3(1):26–33. doi:10.1016/j.jot.2014.07.005
41. Zheng J, Shi L, Liang F, et al. Sirt3 ameliorates oxidative stress and mitochondrial dysfunction after intracerebral hemorrhage in diabetic rats. *Front Neurosci*. 2018;12:414. doi:10.3389/fnins.2018.00414
42. Yan J, Xu W, Lenahan C, et al. Met-RANTES preserves the blood-brain barrier through inhibiting CCR1/SRC/Rac1 pathway after intracerebral hemorrhage in mice. *Fluids Barriers CNS*. 2022;19(1):7. doi:10.1186/s12987-022-00305-3
43. Tschoe C, Bushnell CD, Duncan PW, Alexander-Miller MA, Wolfe SQ. Neuroinflammation after intracerebral hemorrhage and potential therapeutic targets. *J Stroke*. 2020;22(1):29–46. doi:10.5853/jos.2019.02236
44. Xiao L, Zheng H, Li J, Wang Q, Sun H. Neuroinflammation mediated by NLRP3 inflammasome after intracerebral hemorrhage and potential therapeutic targets. *Mol Neurobiol*. 2020;57(12):5130–5149. doi:10.1007/s12035-020-02082-2
45. Fang H, Wang PF, Zhou Y, Wang YC, Yang QW. Toll-like receptor 4 signaling in intracerebral hemorrhage-induced inflammation and injury. *J Neuroinflammation*. 2013;10:27. doi:10.1186/1742-2094-10-27
46. Guo H, Zhang Y, Hu Z, Wang L, Du H. Screening and identification of biomarkers associated with the immune infiltration of intracerebral hemorrhage. *J Clin Lab Anal*. 2022;36(5):e24361. doi:10.1002/jcla.24361
47. Yan K, Zhang R, Sun C, et al. Bone marrow-derived mesenchymal stem cells maintain the resting phenotype of microglia and inhibit microglial activation. *PLoS One*. 2013;8(12):e84116. doi:10.1371/journal.pone.0084116
48. Ding R, Li H, Liu Y, et al. Activating cGAS-STING axis contributes to neuroinflammation in CVST mouse model and induces inflammasome activation and microglia pyroptosis. *J Neuroinflammation*. 2022;19(1):137. doi:10.1186/s12974-022-02511-0
49. Jin M, Shiwaku H, Tanaka H, et al. Tau activates microglia via the PQBP1-cGAS-STING pathway to promote brain inflammation. *Nat Commun*. 2021;12(1):6565. doi:10.1038/s41467-021-26851-2
50. Balka KR, De Nardo D. Molecular and spatial mechanisms governing STING signalling. *FEBS J*. 2021;288(19):5504–5529. doi:10.1111/febs.15640
51. Li T, Lu L, Pember E, Li X, Zhang B, Zhu Z. New insights into neuroinflammation involved in pathogenic mechanism of alzheimer's disease and its potential for therapeutic intervention. *Cells*. 2022;11:12.